Article

Hydrogen-Bonding Motifs in Piperazinediium Salts

Chris S. Hawes [1], Cherry Chen [2], Andrew Tran [2] and David R. Turner [1],*

[1] School of Chemistry, Monash University, Clayton, VIC 3800, Australia;
   E-Mail: chris.hawes@monash.edu

[2] Penleigh and Essendon Grammar School, P.O. Box 417, Niddrie, VIC 3042, Australia

* Author to whom correspondence should be addressed; E-Mail: david.turner@monash.edu;
   Tel.: +61-03-9905-6293; Fax: +61-03-9905-4597.

Abstract: Four novel organic salts of piperazine and 2-methylpiperazine with *p*-toluenesulfonic acid and chloroacetic acid have been synthesized and structurally characterized. The hydrogen-bonding ring synthons that exist between the cation/anion pairs are compared and contrasted alongside database results.

Keywords: hydrogen bonding; supramolecular synthon; crystallography; piperazine

1. Introduction

Hydrogen bonding interactions are amongst the most useful supramolecular interactions in crystal engineering due to their directionality and relatively strong associations [1,2]. These properties are frequently observed to give semi-reproducible hydrogen bonding synthons and give rise to the hope of predictably forming desired solid-state architectures [3–5]. Such interactions are typically explored through crystallographic studies, with complementary methods such as NMR and computational approaches also utilized [6–10].

Particularly strong hydrogen bonding interactions are formed when charged species are used as the donor and acceptor species, as highlighted in a review by Ward and co-workers [11]. Typically this can be achieved by the combination of a charged ammonium cation (or another protonated nitrogen species) as the donor and an anionic group as the acceptor.

Piperazine, and derivatives thereof, have the potential to form dicationic species that are of interest in crystal engineering as they are able to form hydrogen bonds in multiple directions and are rigid cations.

Piperazine is also of interest in medicine as an anti-helmintic, particularly as its citrate and adipate salts, and is also a key component of many other pharmaceuticals. Many structures have been reported containing the piperazinediium cation, likely a result of its use as a base during syntheses. In addition, a number of carboxylate salts have been reported including the series $CH_3(CH_2)_xCO_2^-$ ($x = 0$–3, 5, 6, 8, 10, 12, 14) [12–14] and $^-O_2C(CH_2)_xCO_2^-$ ($x = 1$–4, 6) [15–19]. A recurring motif that is observed in both of these series of structures is the $R_4^4(18)$ ring (using Graph-Set analysis) [20,21] formed between two cations and two anions (Figure 1a). There are two ring motifs involving piperazinediium/carboxylates that can give rise to 1D hydrogen-bonded chains which vary by the manner in which the cations bridge between anions (Figure 1). A search of the Cambridge Structural Database reveals that there are marginally more structures reported with the larger $R_4^4(18)$ ring than with the smaller $R_4^4(12)$ ring with 29 and 19 reported entries, respectively [22,23].

Structures of 2-methylpiperazinediium are considerably rarer than those of piperazinediium, particularly as simple salts. Enantiomerically pure tartrate salts, in both 1:1 and 1:2 anion:cation ratios, have been reported as monohydrates [24,25] which prevents direct comparison with the non-hydrated piperazine analogues [26,27]. The structure of 2-methylpiperazinediium trichloroacetate has also been reported, although the piperazine analogue has not been [28].

Herein we report the structures of four novel organic salts of piperazine and racemic 2-methylpiperazine with *p*-toluenesulfonic acid and chloroacetic acid and explore the similarities and differences in the intermolecular interactions that are observed.

Figure 1. Two hydrogen bonding motifs between piperazinediium and carboxylates; an $R_4^4(18)$ ring (**a**) and a smaller $R_4^4(12)$ ring (**b**). The protonated piperazine rings are shown side-on for clarity.


(**a**)   (**b**)
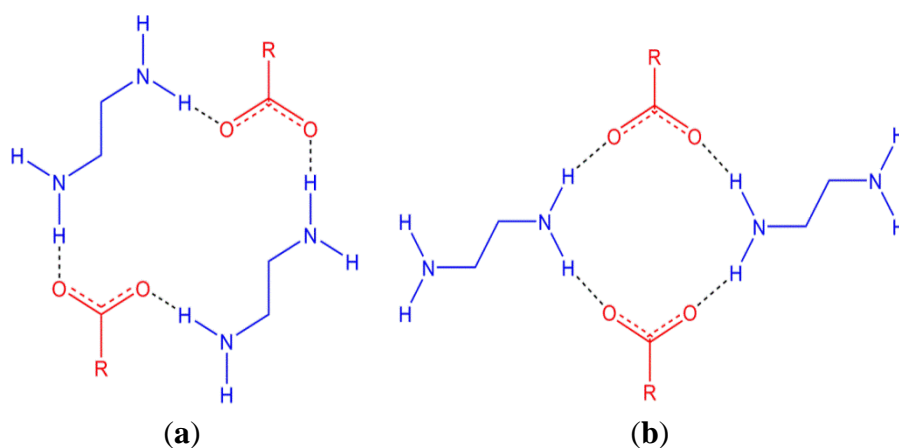
2. Results and Discussion

The four compounds studied are the salt combinations formed using piperazine (pip) and ±2-methylpiperazine (Mepip) as bases in reactions with *p*-toluenesulfonic acid (TSOH) and chloroacetic acid (ClAcOH). All compounds, (pipH$_2$)(TsO)$_2$ (**1**), (MepipH$_2$)(TsO)$_2$ (**2**), (pipH$_2$)(ClAcO)$_2$ (**3**) and (MepipH$_2$)(ClAcO)$_2$ (**4**), were crystallized from concentrated aqueous solutions containing a 1:2 mixture of base and acid in quantitative yields (Figure 2). Comparison of powder X-ray diffraction

traces with those calculated from single crystal data shows that all the compounds form as pure phases (see Experimental Section).

Figure 2. The bases and acids used in this study.

pip   Mepip   TsOH   ClOAcH
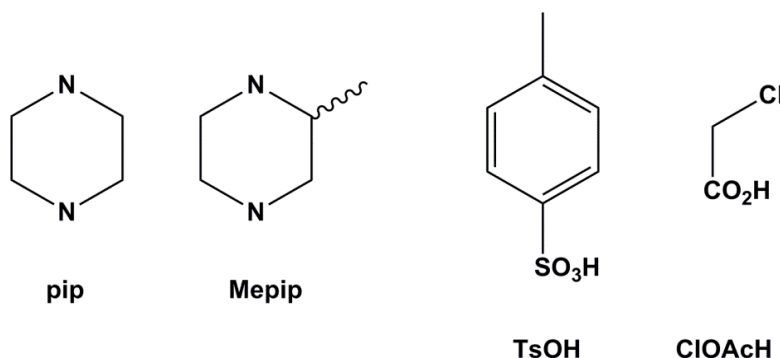
2.1. p-Toluenesulfonate Structures

The structures obtained using *p*-toluenesulfonate as the anion contains the expected NHO interactions although, perhaps unexpectedly, not all of the oxygen atoms are involved in these interactions. In both instances the compounds form one-dimensional hydrogen-bonding chains with additional weaker interactions between these chains. The chains have different molecular arrangements and different hydrogen bonding patterns.

The compound (pipH$_2$)(TsO)$_2$ (**1**) crystallizes in the space group *P*-1 with one formula unit in the ASU, consisting of two *p*-toluenesulfonate anions and half of each of the two crystallographically unique piperazinediium cations. The cation/anion pairs form one-dimensional hydrogen-bonding chains that propagate parallel to the crystallographic *c*-axis (Figure 3a). The 1D chain contains the less common R$_4^4$(12) motif, with the long axis of the cations approximately aligned along the chain. The geometries of the hydrogen bonds in the structure are quite diverse considering that all are between identical chemical moieties with H$\cdots$A distances in the range 1.84–2.10 Å and D–H$\cdots$A angles in the range 146°–174° (Table 1). The longest and least direction of these interactions (N1$\cdots$O1) appears to be due to the presence of a second, much weaker, interaction between the same proton and a second oxygen atom of the cation (O2) giving rise to a distorted bifurcated interaction. There is also a long and less linear H$\cdots$O interaction between adjacent chains parallel to the *ac*-plane which gives a weakly joined 2D network (N1$\cdots$O6). These 2D sheets interdigitate with weak methyl CH$\cdots\pi$ interactions between the layers.

The methyl-substituted analogue, (MepipH$_2$)(TsO)$_2$, crystallizes in the space group *Pc*, with a half occupancy water site present in the ASU alongside two anions and one cation (**2**). As with **1** the dominant hydrogen-bonding interactions form a one-dimensional chain, although in this case the repeating synthon is the R$_4^4$(18) ring (Figure 3b, *cf.* Figure 1). The hydrogen bonds in this chain have H$\cdots$A distances in the range 1.91–2.00 Å and D–H$\cdots$A angles in the range 143°–158° (Table 1) which are considerably smaller ranges than those observed in the structure of **1**. There are longer and less linear interactions between the 1D chains with each of the NH$_2$ groups forming an R$_2^2$(6) ring with a sulfonate in a neighboring chain, giving rise to 2D sheets. These sheets interdigitate with aryl CH$\cdots\pi$ interactions between the layers. The 50% occupancy water molecules reside between sulfonate groups on the periphery of the 2D sheets with O$\cdots$O distances of *ca.* 2.8 Å, suggesting that there may be hydrogen

bonding interactions present (Figure 3c) (note: the hydrogen atoms of the partial occupancy water could not be experimentally located from the Fourier difference map). Crystallinity is lost upon heating and removal of the water molecule. Whilst both enantiomers of the cation are present in the crystal structure, with the presence of a glide plane, the non-centrosymmetry arises from the packing in which all methyl groups are orientated in one direction with respect to the *a* axis. The compound may potentially display piezoelectric properties as observed in the closely related (R-H$_2$Mepip)(CCl$_3$CO$_2$) [28].

It is interesting that such a minor difference in the cation, the addition of a methyl group, changes the predominant hydrogen-bonding motif, although the effects of the small amount of lattice solvent cannot be ignored. A possible reason is that there is increased steric bulk associated with the methyl group and in combination with the SO$_3$ group this requires a different orientation of the cation to provide efficient packing and favorable interactions, although further studies are required to analyse any potential effect in detail.

Figure 3. (**a**) Views perpendicular to and along part of the 1D hydrogen bonding chain in the structure of (pipH$_2$)(TsO)$_2$ (**1**); (**b**) Views perpendicular to and along part of the 1D hydrogen bonding chain in the structure of (MepipH$_2$)(TsO)$_2$ ½H$_2$O (**2**); (**c**) Packing diagram of (MepipH$_2$)(TsO)$_2$ ½H$_2$O showing the accentricity and the location of the water molecules (in green).
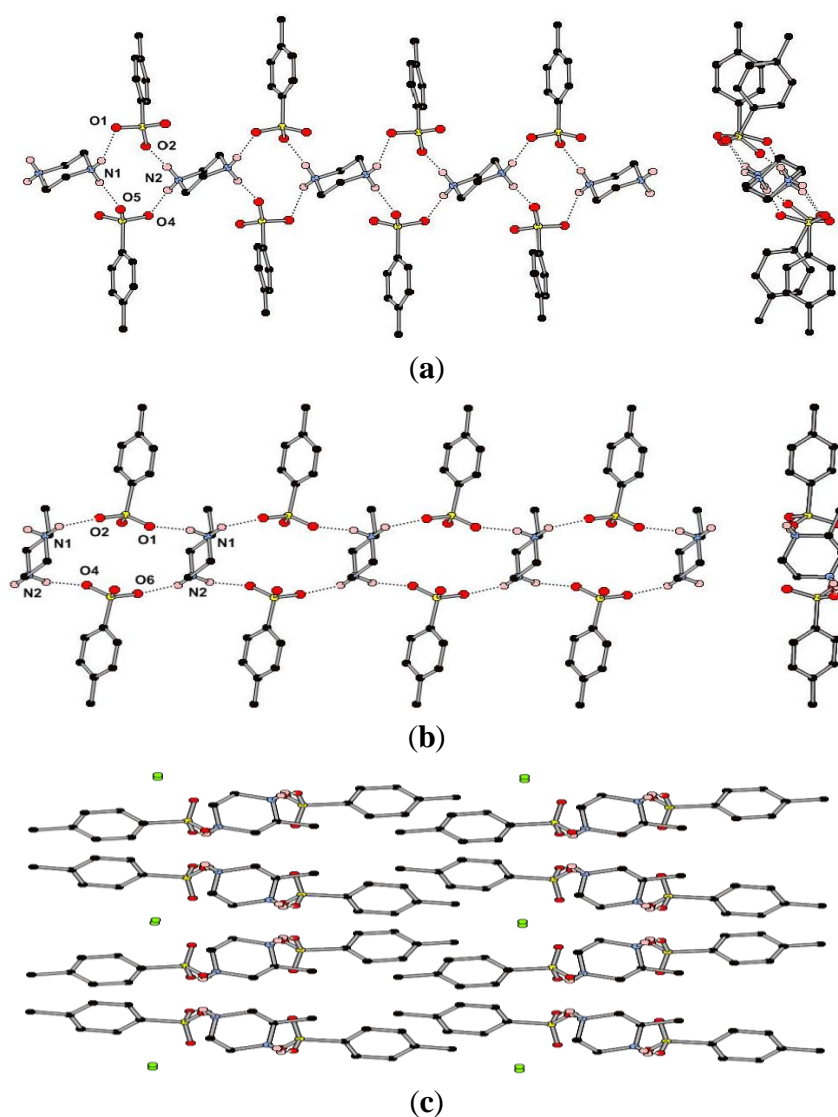

(**a**)

(**b**)

(**c**)

Table 1. Hydrogen-bonding parameters for compounds **1** and **2**. Symmetry equivalents used: #1, $x + 1$, y, z; #2, $x - 1$, y, z; #3, x, y, $z - 1$; #4, x, y, $z - \frac{1}{2}$; #5, x, $1 - y$, $z + \frac{1}{2}$; #6, x, $1 - y$, $z - \frac{1}{2}$.

	1				**2**		
Interaction	**D$\cdots$A (Å)**	**H$\cdots$A (Å)**	**D–H$\cdots$A (°)**	**Interaction**	**D$\cdots$A (Å)**	**H$\cdots$A (Å)**	**D–H$\cdots$A (°)**
N1$\cdots$O1	2.9126(16)	2.10	146.3	N1$\cdots$O2#3	2.790(5)	2.00	143.0
N1$\cdots$O5#1	2.8089(17)	1.89	174.1	N1$\cdots$O1#4	3.076(6)	2.41	129.0
N2$\cdots$O2#2	2.7223(17)	1.84	159.5	N1$\cdots$O1	2.798(5)	1.92	158.0
N2$\cdots$O4	2.7542(15)	1.86	163.0	N1$\cdots$O2#4	3.063(5)	2.50	120.0
N1$\cdots$O2	3.0536(15)	2.50	114.9	N2$\cdots$O6#5	2.772(5)	1.98	142.9
N1$\cdots$O6	2.8620(16)	2.30	114.9	N2$\cdots$O4	3.080(5)	2.42	128.8
–	–	–	–	N2$\cdots$O4#6	2.784(5)	1.91	157.3
–	–	–	–	N2$\cdots$O6	3.149(6)	2.57	121.0

2.2. Chloroacetate Structures

As with the *p*-toluenesulfonate structures, those obtained using the chloroacetate anion showed the expected NH$\cdots$O interactions. However, in contrast to the structures of **1** and **2**, the structures of (pipH$_2$)(ClAcO)$_2$ (**3**) and (MepipH$_2$)(ClAcO)$_2$ (**4**) display similar hydrogen-bonding motifs.

Compound **3** crystallizes in the space group *P*-1 with one chloroacetate anion and half of a piperazinediium cation in the asymmetric unit. The ions arrange to form a 1D hydrogen-bonded chain containing the R$_4^4$(18) ring (Figure 4a). There are only two crystallographically unique hydrogen bonds in the structure which have similar geometric parameters (Table 2). In contrast to the structures of **1** and **2**, there are no additional hydrogen bonds between the chains in **3**, presumably due to there being less acceptor sites in the anion. The only tentative interaction appears to be a close contact between the chlorine atoms of nearby anions with a Cl$\cdots$Cl distance of *ca.* 3.3 Å which is within the sum of the van der Vaals radii, and a C–Cl$\cdots$Cl angle of 151 °[29–31]. These geometric parameters are in excellent agreement with those set out by Awwadi *et al.* [32,33] based on database and computational studies, for halogen bonding between sp^3 hybridized carbon-halogen groups and are classified as "type I" halogen$\cdots$halogen interactions.

The methylated analogue, compound **4**, crystallizes in the monoclinic space group *P*2$_1$/*c* with a complete formula unit in the ASU. The structure contains one-dimensional hydrogen-bonding chains that are very similar to those in the structure of **3** and again display the R$_4^4$(18) ring motif (Figure 4b). Indeed, the similarity between the structures of **3** and **4** is reflected in the similar cell parameters (see experimental details). The hydrogen bonding interactions in **4** appear marginally shorter and more linear than those in **3**, although there is obvious uncertainty in proton position from X-ray data. Whilst the overall structure is centrosymmetric, each chain contains only one isomer of 2-methylpiperazinediium. There are no hydrogen bonding interactions between the chains, with the only noteworthy close interaction being between Cl2 and its symmetry generated equivalent with a Cl$\cdots$Cl interaction with very similar geometric parameters to those observed in **3**. The second crystallographically unique anion does not have a corresponding close contact. In systems **3** and **4** it appears that the presence of a methyl substituent does not significantly alter the structure, with only very minor differences observed between the hydrogen bonding geometries.

Figure 4. (**a**) Views perpendicular to and along part of the 1D hydrogen bonding chain in the structure of (pipH$_2$)(ClOAc)$_2$ (**3**); (**b**) Views perpendicular to and along part of the 1D hydrogen bonding chain in the structure of (MepipH$_2$)(ClOAc)$_2$ (**4**); (**c**) The Cl···Cl interaction between adjacent chloroacetate anions in the structures of **3** and **4**.
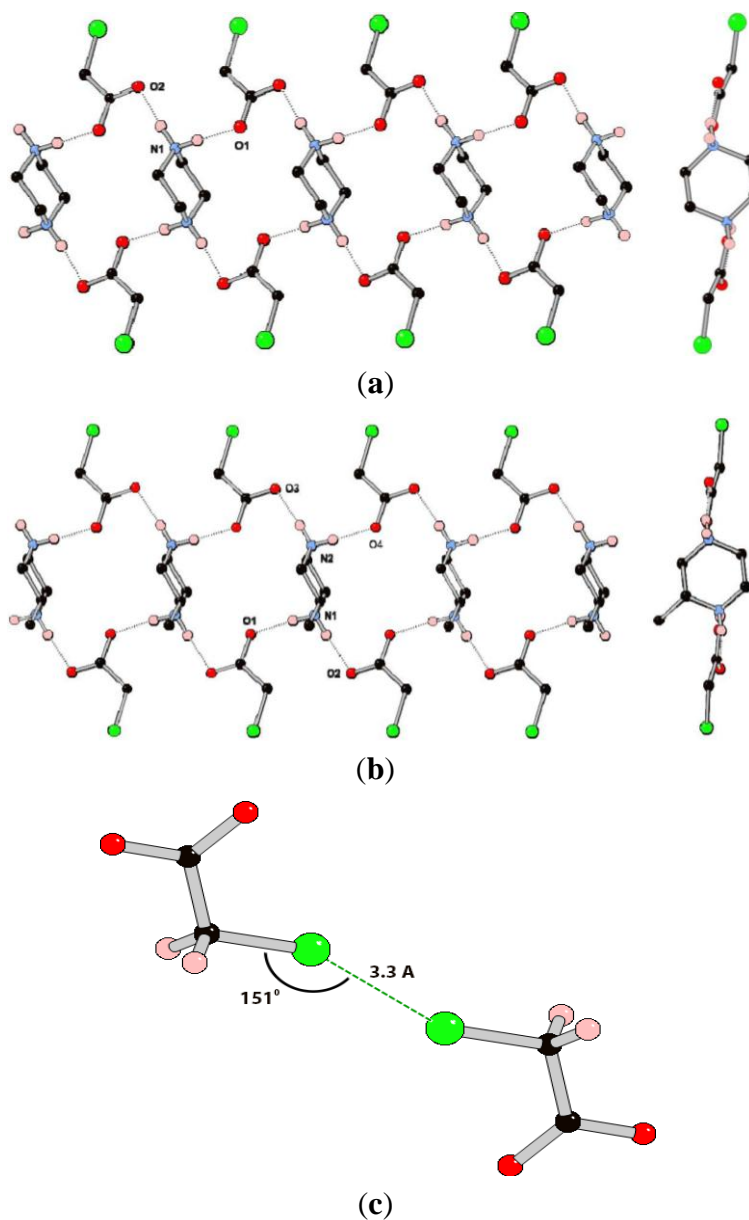

(**a**)

(**b**)

(**c**)

Table 2. Hydrogen-bonding parameters for compounds **3** and **4**. Symmetry equivalents used: #1, $x + 1$, y, z; #2, $x - 1$, y, z.

3				4			
Interaction	**D···A (Å)**	**H···A (Å)**	**D-H···A (°)**	**Interaction**	**D···A (Å)**	**H···A (Å)**	**D-H···A (°)**
N1···O2	2.7517(17)	1.85	165.6	N1···O1	2.741(2)	1.76	172.4
N1···O1#1	2.6915(16)	1.78	169.2	N1···O2#2	2.741(2)	1.76	171.7
–	–	–	–	N2···O3	2.727(2)	1.75	169.8
–	–	–	–	N2···O4#2	2.713(2)	1.73	174.8

3. Experimental Section

3.1. Synthesis

All materials were purchased from Sigma-Aldrich, Castle Hill, Australia and used without further purification. All compounds were synthesized by slow evaporation of a 2 mL aqueous solution containing the base (0.050 g) with two molar equivalents of the acid. Gentle heating was used where necessary to ensure full dissolution. All compounds were obtained as colorless crystals in near quantitative yields. The purity of all four crystalline compounds was determined by powder X-ray diffraction (Bruker AXS, Madison, WI, USA). Comparisons between calculated and experimentally determined patterns are shown in Figure 5.

Figure 5. Comparison of experimental (298 K) and calculated (100 K) powder X-ray diffraction data for compounds **1**–**4**. All compounds show good agreement, allowing for minor differences resulting from temperature, with preferred orientation of the experimental sample evident in all cases.
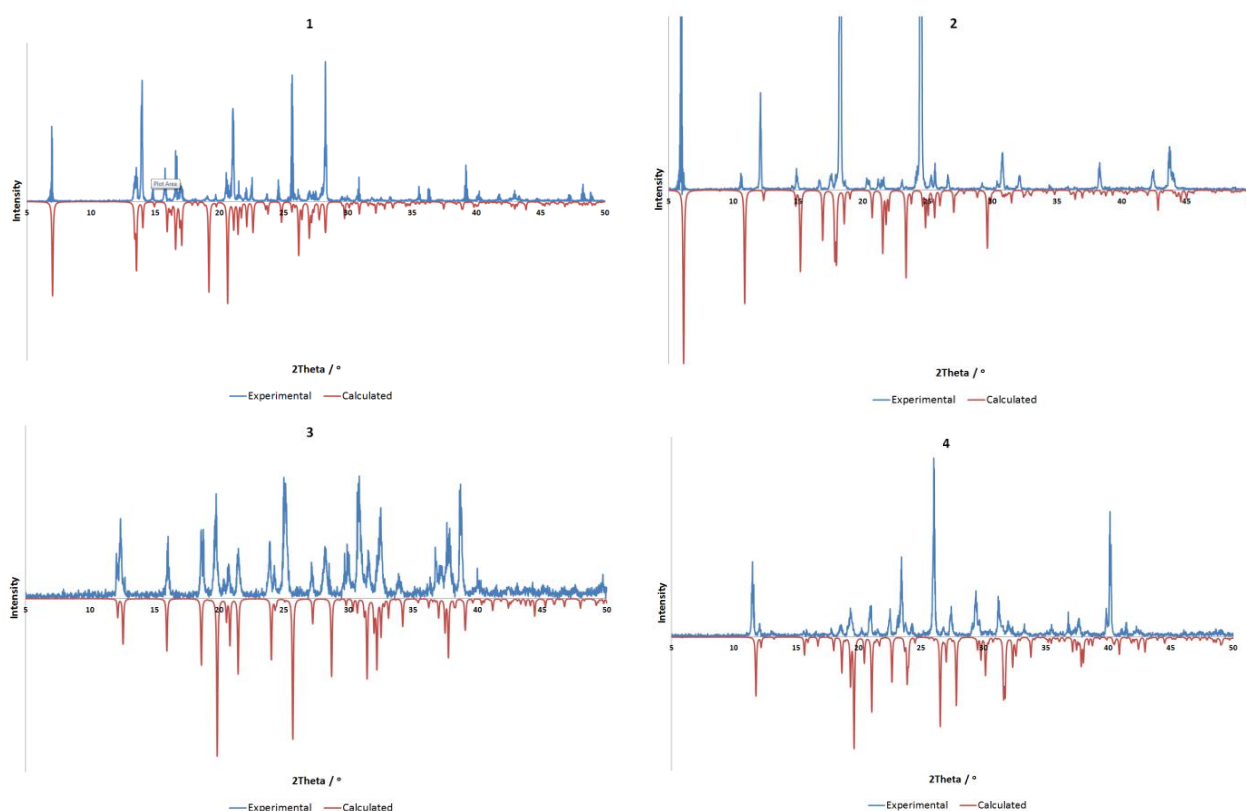
Piperazine-1,4-diium *p*-tolylsulfonate (**1**): m.p. > 300 °C. FTIR (v/cm^{-1}): 2960 w, 2799 w, 1602 m, 1440 m sh, 1394 m, 1319 w, 1220 s, 1154 m, 1125 s, 1029 s, 1006 s, 809 s, 671 s.

±2-Methylpiperazine-1,4-diium p-tolylsulfonate (**2**): m.p. 254–257 °C. FTIR (v/cm^{-1}): 3050 m, 2827 w, 1567 w, 1435 m, 1172 s sh, 1104 s, 1040 s, 1010 m, 972 m, 952 m, 898 w, 847 w, 814 m, 672 s.

Piperazine-1,4-diium chloroacetate (**3**): m.p. 158–159 °C. FTIR (v/cm^{-1}): 2672 m br, 2375 m br, 1641 w, 1587 s, 1456 m, 1395 s, 1378 s, 1304 m, 1256 s, 1219 w, 1084 m, 1016 m, 932 m, 770 s, 668 s.

±2-Methylpiperazine-1,4-diium chloroacetate (**4**): m.p. 161–162 °C. FTIR (v/cm^{-1}): 2962 w, 2351 s br, 1641 m, 1567 s, 1496 m, 1456 m, 1388 s, 1310 w, 1266 s, 1135 m, 1087 m, 1047 m, 1030 m, 932 s, 773 s, 668 s.

3.2. X-Ray Crystallography

Crystals were mounted on a nylon loop using viscous hydrocarbon oil. Data for all compounds were collected using the MX1 beamline at the Australian Synchrotron operating at 17.4 keV ($\lambda = 0.7107$ Å). Data collection temperatures were maintained at 100 K using an open-flow N_2 cryostream. Data collection was conducted using the BluIce interface program. Data indexing and reduction was conducted using the program XDS [34]. All structures were solved by direct methods using SHELXS-2013 [35]. Structures were refined using full-matrix least squares against F^2 using SHELXL-2013 with the program X-Seed as a graphical interface [36]. All non-hydrogen atoms were refined using an anisotropic model. Hydrogen atoms were placed in idealized X-ray positions and refined using a riding model. Hydrogen atoms on the partial occupancy water in the structure of **2** could not be located in the Fourier map but are included in all calculations. Full crystallographic data are given in Table 3. Data are deposited with the Cambridge Structural Database (CCDC 980166–980169 for **1**–**4**, respectively). Data can be obtained for free from www.ccdc.cam.ac.uk

Table 3. Crystallographic and refinement data for compounds **1**–**4**.

Compound	1 AT10	2 CC10	3 AT14	4 CC14
Formula	(H$_2$Pip)(TsO)$_2$	(H$_2$MePip)(TsO)$_2$ ½H$_2$O	(H$_2$Pip)(OAcCl)$_2$	(H$_2$MePip)(OAcCl)$_2$
Empirical Formula	C$_{18}$H$_{26}$N$_2$O$_6$S$_2$	C$_{19}$H$_{29}$N$_2$O$_{6.5}$S$_2$	C$_8$H$_{16}$Cl$_2$N$_2$O$_4$	C$_9$H$_{18}$Cl$_2$N$_2$O$_4$
Formula Mass	430.53	453.56	275.13	289.15
Crystal System	Triclinic	Monoclinic	Triclinic	Monoclinic
Space Group	*P*-1	*Pc*	*P*-1	*P2$_1$/c*
a/Å	5.9020(12)	14.584(3)	5.6260(11)	5.7050(11)
b/Å	13.059(3)	9.863(2)	7.2100(14)	29.975(6)
c/Å	13.581(3	7.6460(15)	7.5280(15)	7.5280(15)
α/°	73.55(3)	90	77.60(3)	90
β/°	86.00(3)	100.89(3)	80.83(3)	97.26(3)
γ/°	84.09(3)	90	85.29(3)	90
V/Å^3	997.7(3)	1080.0(4)	294.07(10)	1277.0(4)
μ/mm^{-1}	0.305	0.284	0.553	0.514
Refs. Collected	36824	11230	11028	23550
Theta Range	1.56–31.54	2.71–31.50	2.80–31.49	1.36–31.51
Unique Refs. (R$_{int}$)	5606 (0.0660)	5649 (0.0779)	1660 (0.0706)	3548 (0.0460)
Obs. Refs. (I > 2σI)	5391	5038	1557	3414
R1 (I > 2σI/all data)	0.0386/0.0399	0.0786/0.0834	0.0361/0.0379	0.0473/0.0486
wR2 (I > 2σI/all data)	0.1027/0.1040	0.2118/0.2184	0.0940/0.0950	0.1130/0.1137
GooF	1.077	1.081	1.120	1.122

X-ray powder diffraction (XRPD) data was collected at room temperature using a Bruker X8 instrument equipped with Cu kα radiation ($\lambda = 1.54$ Å).

4. Conclusions

Four salts containing the dication of piperazine (pipH$_2$) or its 2-methyl derivative (MepipH$_2$) with *p*-toluenesulfonate (TsO) and chloroacetate (ClAcO) have been prepared and structurally characterized to examine the hydrogen-bonding motifs that are present. All four compounds, (pipH$_2$)(TsO)$_2$ (**1**), (MepipH$_2$)(TsO)$_2$ (**2**), (pipH$_2$)(ClAcO)$_2$ (**3**) and (MepipH$_2$)(ClAcO)$_2$ (**4**), contain one-dimensional hydrogen bonding chains as the primary structural feature. These chains contain the less common R$_4^4$(12) motif in **1** and the more common R$_4^4$(18) motif in **2**–**4** (as ascertained by searches of the CSD). In the structures of **1** and **2** there is additional, weak hydrogen bonding between the chains that is absent in **3** and **4** due to the larger number of acceptor atoms present in the sulfonate *versus* the carboxylate. In the chloroacetate structures, the presence of a methyl group does not affect the hydrogen bonding motif that is observed, whereas in the toluenesulfonate structures it does appear that there is some influence, possibly due to the larger bulk of sulfonate compared to carboxylate. Combined with CSD searches, these results suggest that the 1D chain based on R$_4^4$(18) hydrogen-bonding motifs is quite a stable supramolecular synthons and future work aims to exploit this in crystal engineering applications. Such applications involve the use of rigid polycarboxylates to construct per-designed network architectures, exploring the physical properties of materials containing different synthons (with potential pharmaceutical relevance) and exploring effects such as piezoelectricity in engineered non-centrosymmetric networks of 2-methylpiperazine.

Conflicts of Interest

The authors declare no conflict of interest.

References

1. Steed, J.W.; Atwood, J.L. *Supramolecular Chemistry*, 2nd ed.; John Wiley & Sons: Chichester, UK, 2009.
2. Steed, J.W.; Turner, D.R.; Wallace, K.J. *Core Concepts in Supramolecular Chemistry and Nanochemistry*; John Wiley: Chichester, UK; Hoboken, NJ, USA, 2007.
3. Burrows, A.D. Crystal engineering using multiple hydrogen bonds. *Struct. Bond.* **2004**, *108*, 55–95.
4. Etter, M.C. Hydrogen-bonds as design elements in organic-chemistry. *J. Phys. Chem.* **1991**, *95*, 4601–4610.
5. Jeffrey, G.A. *An Introduction to Hydrogen Bonding*; OUP USA: New York, NY, USA, 1997.
6. Spackman, M.A.; Jayatilaka, D. Hirshfeld surface analysis. *CrystEngComm* **2009**, *11*, 19–32.
7. Yates, J.R.; Pham, T.N.; Pickard, C.J.; Mauri, F.; Amado, A.M.; Gil, A.M.; Brown, S.P. An investigation of weak CH$\cdots$O hydrogen bonds in maltose anomers by a combination of calculation and experimental solid-state NMR spectroscopy. *J. Am. Chem. Soc.* **2005**, *127*, 10216–10220.

8. Chierotti, M.R.; Gobetto, R. NMR crystallography: The use of dipolar interactions in polymorph and co-crystal investigation. *CrystEngComm* **2013**, *15*, 8599–8612.

9. Mafra, L.; Santos, S.M.; Siegel, R.; Alves, I.; Almeida Paz, F.A.; Dudenko, D.; Spiess, H.W. Packing interactions in hydrated and anhydrous forms of the antibiotic ciprofloxacin: A solid-state NMR, X-ray diffraction, and computer simulation study. *J. Am. Chem. Soc.* **2011**, *134*, 71–74.

10. Saleh, G.; Gatti, C.; LoPresti, L.; Contreras-García, J. Revealing non-covalent interactions in molecular crystals through their experimental electron densities. *Chemistry* **2012**, *18*, 15523–15536.

11. Ward, M.D. Design of crystalline molecular networks with charge-assisted hydrogen bonds. *Chem. Commun.* **2005**, *47*, 5838–5842.

12. Brisse, F.; Denault, J.; Sangin, J.P. Study of aliphatic chain compounds 1. Synthesis and crystallographic characterization of bis (*n*-alkanoates) of piperazinium, $2[C_xH_{2x-1}O_2^-][C_4H_{12}N_2^{2+}]$. *J. Appl. Crystallogr.* **1982**, *15*, 279–281.

13. Brisse, F.; Sangin, J.P. Study of compounds with aliphatic chains 2. The structure of piperazinium bis(normal-dodecanoate). *Acta Crystallogr. Sect. B* **1982**, *38*, 215–221.

14. Venkatramani, L.; Craven, B.M. Disordered fatty-acid chains in piperazinium myristate and palmitate. *Acta Crystallogr. Sect. B* **1991**, *47*, 968–975.

15. Ponomarev, V.I.; Klimchuk, E.G.; Merzhanov, A.G.; Filipenko, O.S. Structural-chemical transformations during organic self-propagating high-temperature synthesis. Crystal structure of piperazine malonate and its crystal hydrate. *Russ. Chem. B.* **1997**, *46*, 939–943.

16. Vanier, M.; Belangergariepy, F.; Brisse, F. Structural studies of compounds with aliphatic chains 10. Structure of piperazinium suberate monohydrate, $[C_8H_{12}O_4^{2-}][C_4H_{12}N_2^{2+}]H_2O$. *Acta Crystallogr. Sect. C* **1983**, *39*, 916–917.

17. Vanier, M.; Brisse, F. Structural studies of compounds with aliphatic chains 7. The structure of piperazinium glutarate and the geometry of the piperazinium cation. *Acta Crystallogr. Sect. B* **1982**, *38*, 3060–3063.

18. Vanier, M.; Brisse, F. Structural studies of compounds with aliphatic chains 8. Structure of piperazinium succinate, $[C_4H_4O_4^{2-}][C_4H_{12}N_2^{2+}]$. *Acta Crystallogr. Sect. C* **1983**, *39*, 912–914.

19. Vanier, M.; Brisse, F. Structural studies of compounds with aliphatic chains 9. Structure of piperazinium adipate, $[C_6H_8O_4^{2-}][C_4H_{12}N_2^{2+}]$. *Acta Crystallogr. Sect. C* **1983**, *39*, 914–915.

20. Bernstein, J.; Davis, R.E.; Shimoni, L.; Chang, N.L. Patterns in hydrogen bonding—Functionality and graph set analysis in crystals. *Angew. Chem. Int. Ed.* **1995**, *34*, 1555–1573.

21. Etter, M.C.; Macdonald, J.C.; Bernstein, J. Graph-set analysis of hydrogen-bond patterns in organic-crystals. *Acta Crystallogr. Sect. B* **1990**, *46*, 256–262.

22. Allen, F.H. The cambridge structural database: A quarter of a million structures and rising. *Acta Crystallogr. Sect. B* **2002**, *B58*, 380–388.

23. Cambridge Structural Database. Version 5.31 + 1 update. February 2012.

24. Katagiri, H.; Morimoto, M.; Sakai, K. A pair of diastereomeric 1:1 salts of (s)- and (r)-2-methylpiperazine with (2s,3s)-tartaric acid. *Acta Crystallogr. Sect. C* **2009**, *65*, O357–O360.

25. Katagiri, H.; Morimoto, M.; Sakai, K. A pair of diastereomeric 1:2 salts of (r)- and (s)-2-methylpiperazine with (2s,3s)-tartaric acid. *Acta Crystallogr. Sect. C* **2010**, *66*, O20–O24.

26. Aakeroy, C.B.; Bahra, G.S.; Nieuwenhuyzen, M. Piperazinium *l*-tartrate. *Acta Crystallogr. Sect. C* **1996**, *52*, 1471–1473.

27. Farrell, D.M.M.; Ferguson, G.; Lough, A.J.; Glidewell, C. Chiral *versus* racemic building blocks in supramolecular chemistry: Tartrate salts of organic diamines. *Acta Crystallogr. Sect. B* **2002**, *58*, 272–288.

28. Cai, H.-L.; Zhang, T.; Chen, L.-Z.; Xiong, R.-G. The first homochiral compound with temperature-independence of piezoelectric properties. *J. Mater. Chem.* **2010**, *20*, 1868–1870.

29. Bondi, A. Van der waals volumes + radii. *J. Phys. Chem.* **1964**, *68*, 441–451.

30. Metrangolo, P.; Meyer, F.; Pilati, T.; Resnati, G.; Terraneo, G. Halogen bonding in supramolecular chemistry. *Angew. Chem. Int. Ed.* **2008**, *47*, 6114–6127.

31. Rissanen, K. Halogen bonded supramolecular complexes and networks. *CrystEngComm* **2008**, *10*, 1107–1113.

32. Awwadi, F.F.; Willett, R.D.; Peterson, K.A.; Twamley, B. The nature of halogen $\cdots$ halogen synthons: Crystallographic and theoretical studies. *Chemistry* **2006**, *12*, 8952–8960.

33. Metrangolo, P.; Resnati, G. Type II halogen $\cdots$ halogen contacts are halogen bonds. *IUCrJ* **2013**, *1*, 5–7.

34. Kabsch, W. Automatic processing of rotation diffraction data from crystals of initially unknown symmetry and cell constants. *J. Appl. Cryst.* **1993**, *26*, 795–800.

35. Sheldrick, G.M. A short history of SHELX. *Acta Crystallogr. Sect. A* **2008**, *64*, 112–122.

36. Barbour, L.J. X-Seed—A software tool for supramolecular crystallography. *J. Supramol. Chem.* **2001**, *1*, 189–191.